Original Article
Advanced oxidation protein products accelerated the bone loss and weakened bone strength in ovariectomised rats

Shuai Zheng[1*], Shuai Qin[1,2*], Zhao-Ming Zhong[1], Qian Wu[1], Zheng Wang[1], Jian-Ting Chen[1]

[1]Department of Orthopedic Spinal Surgery, Nanfang Hospital, Southern Medical University, Guangzhou, China;
[2]Department of Ophthalmology, The People's Hospital of Zhuhai, Zhuhai, Guangdong, China. *Equal contributors.

Abstract: Introduction: Advanced oxidation protein products (AOPPs) are prevalent in several kinds of disorders. Previous research revealed that the levels of AOPPs in postmenopausal women were significantly higher than that in premenopausal women. Whether AOPPs have any effect on bone loss remains unclear. Our research analysed the role of AOPPs on the development of osteoporosis in ovariectomised (OVX) rats. Methods: Female SD rats were divided into five groups (SHAM, OVX+PBS, OVX+RSA (Rat Serum Albumin), OVX+AOPPs, OVX+AOPPs+SOD) and subjected to sham or ovariectomy. PBS, RSA, and AOPPs were injected daily with or without intragastric administration of superoxide dismutase (SOD) after surgery. Every 4 weeks blood and the tibia were harvested from eight rats in each group. The expression of osteocalcin and CTX-I (C-terminal crosslinking telopeptide of type I collagen) in serum was measured by ELISA, and the tibiae were subjected to metaphyseal three-point bending and μCT analysis. Results: AOPPs increased the serum level of osteocalcin and CTX-I. μCT showed AOPPs decreased bone mass at week 4 and week 8, while significant differences in F_{max} and energy absorption were found between the PBS and AOPPs groups at week 20 and week 24. No significant differences were found between the AOPPs and AOPPs+SOD groups at any time. Conclusions: AOPPs accelerated the bone loss and weakened bone strength in OVX rats.

Keywords: Advanced oxidation protein products, OVX rat model, oxidative stress, postmenopausal osteoporosis, μCT

Introduction

Osteoporosis is characterised by an imbalance between bone formation and resorption, resulting in a net bone (particularly cancellous) loss and increased fracture incidence [1]. Although the aetiology of osteoporosis is not well understood, previous studies have demonstrated that oxidative stress is involved in its pathogeny [2, 3]. In addition, our preliminary research has proved that oxidative stress is also involved in age-related bone loss and might play an important role in the pathology of age-related bone loss [4].

Oxidative stress, a pathological condition characterised by a disturbance in the prooxidant-antioxidant balance in favour of the former, is involved in the development of many diseases such as chronic obstructive pulmonary disease (COPD) [5], coronary artery disease (CAD) [6],

disuse muscle atrophy [7], and uremia [2]. Reactive oxygen species (ROS), the main cause of oxidative stress, mainly consists of H_2O_2, O_2^-, and OH^-, which were generated by the mitochondrial respiratory chain [8, 9] and the accumulation of which could damage to proteins, lipids, nucleic acids, and other cellular components [10]. Furthermore, studies have indicated that proteins are earlier and more susceptible to oxidative damage than lipids, and therefore, proteins are generally considered to be the main original targets of ROS [11, 12].

Advanced oxidation protein products (AOPPs), first found in the plasma of patients with dialysis [13], are a kind of dityrosine-containing and cross-linking protein products formed during oxidative stress by reaction of plasma albumin with chlorinated oxidants [14]. Increased levels of AOPPs have been found in patients with diabetes [15], metabolic syndrome [16], chronic

inflammatory bowel diseases [17], and obesity [18], implying that the accumulation of AOPPs may be relevant in a series of pathophysiologic conditions. Furthermore, Ahmet et al. [19] reported that AOPP levels in postmenopausal women were significantly elevated compared to that in premenopausal women. The plasma concentration of AOPPs is closely correlated with the level of dityrosine, a marker of oxidised protein, and pentosidine, a marker of protein glycoxidation that is tightly related to oxidative stress [20].

Oxidative damage to proteins is reflected by increased levels of AOPPs, which serve as a novel biomarker of oxidative stress [14]. Besides being a marker of oxidative stress, AOPPs have also been shown to play a significant role as effector molecules in a number of biological events. AOPPs have been reported to induce mesangial cell perturbation through PKC-dependent activation of NADPH oxidase [21], and the accumulation of AOPPs promote NADPH oxidase-dependent podocyte depletion by a p53-Bax apoptotic pathway both in vivo and in vitro [22]. Moreover, AOPPs can inhibit differentiation of preadipocytes and activate inflammation in these cells [23], and we have also demonstrated that AOPPs can inhibit proliferation and differentiation of rat osteoblast-like cells (ROB) cells through the ROS-dependent NF-κB pathway [24].

It is well known that the functional limitation of osteoblasts is one of the most important reasons for osteoporosis; therefore, on the basis of our preliminary studies [24] and increased levels of AOPPs in postmenopausal women [19], we think that the accumulation of AOPPs might be involved in the pathophysiological progress of osteoporosis. However, to our knowledge, there is no information available in the literature regarding the effect of AOPPs on the development of postmenopausal osteoporosis in vivo. Consequently, in this research the OVX rat model was used to detect the effect of AOPPs on the genesis development of osteoporosis.

Methods

AOPPs-RSA preparation and determination

AOPPs-rat serum albumin (RSA) was prepared according to a described procedure with minor modifications [13, 25]. Briefly, RSA solution (20 mg/mL, Sigma, St. Louis, MO) was exposed to 200 mmol/L of HOCL for 30 min at room temperature and then dialysed against phosphate buffer solution (PBS) at 4°C for 24 h to remove free HOCL. Control incubation was performed in native RSA dissolved in PBS alone. All the preparations were passed through a Detoxi-Gel column (Thermo, Cambridge, MA) to remove any endotoxin. An amebocyte lysate assay kit (Sigma) was used to determine the level of endotoxin in AOPPs-RSA and the concentration of endotoxin was below 0.025 EU/mL. AOPP content in the sample was determined as described previously [14]. Briefly, 200 μL of sample or chloramine-T was placed in a 96-well plate, and 20 μL of acetic acid was then added. A microplate reader was used to measure the absorbance at 340 nm immediately. AOPP content in the AOPPs-RSA and unmodified RSA was 40.10±2.23 and 0.12±0.07 μmol/g protein, respectively.

Animals

These methods were carried out in strict accordance with the laboratory animal care guidance regulations of the Ministry of Science and Technology of the People's Republic of China. All the animal protocols were approved by the Committee on the Ethics of Animal Experiments of Southern Medical University. Female Sprague-Dawley rats (8 weeks old, purchased from the Laboratory Animals Center of Southern Medical University) were raised in a 12-h light/dark cycle and given free access to food and tap water. All the rats were subjected to sham or OVX surgery as soon as they were acclimatised to the new situation for 2 weeks. Subsequently, the experimental animals were randomly assigned to five groups (sham, OVX+PBS, OVX+RSA, OVX+AOPPs, OVX+AOPPs+superoxide dismutase [SOD]) according to body weight with daily injection of either PBS (100 mg/kg per day), native RSA (100 mg/kg per day), AOPPs (100 mg/kg per day), or AOPPs (100 mg/kg per day) and intragastric administration of SOD (Sigma Chemical, 100 mg/kg per day) separately [22].

The rats were sacrificed at seven predetermined time points for sham (0, 4, 8, 12, 16, 20 and 24 weeks) and six time points for OVX+ PBS (4, 8, 12, 16, 20 and 24 weeks) and treat-
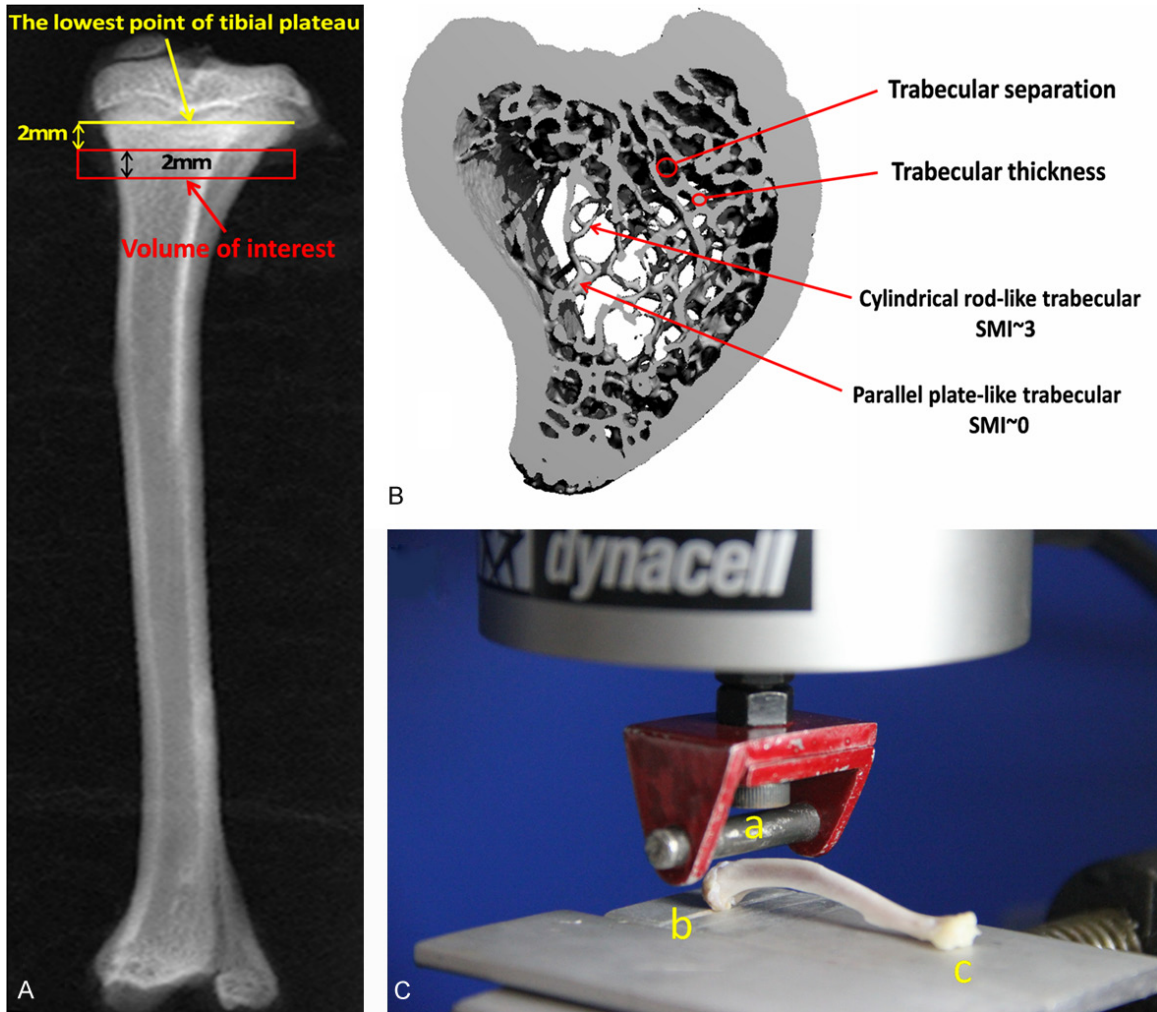
Figure 1. The general introduction of experimental methods of μCT and three-point bending test. A. The volume of interest tested by μCT and three-point bending test. B. Some experimental parameters of rat tibia scanned by μCT. C. The design details of the three-point bending test consisting of the aluminium block and a rounded edge-free notch.

ment (4, 8, 12, 16, 20 and 24 weeks). There were 56 animals in sham groups and 48 animals in the OVX+PBS group and each treatment group. Their bilateral tibias were collected, with soft tissues removed thoroughly, wrapped in normal saline-soaked gauze, and stored at -20°C until used for the research. Both the body and uterine weight were measured at the end of each predetermined time point of the experiment. All animal procedures followed the guidelines of the authors' Intramural Animal Use and Care Committee of Southern Medical University.

Serum biomarker measurements

The blood was collected from the abdominal aorta of rats while they were sacrificed. The serum was separated by centrifugation at 4°C and stored at -80°C until further analysis. Osteocalcin (OC) (bone formation marker) and C-terminal crosslinking telopeptide of type I collagen (CTX-I) (bone resorption marker) in the serum were quantified by OC and CTX-I ELISA kits (Cusabio, Wu Han, China), respectively, according to the manufacturer's protocol. The absorbance at 450 nm was measured by a spectrophotometric plate reader.

Micro-computed tomography analysis

The micro-architecture of the trabecular and cortical bone were assessed using a high resolution micro-CT system (μCT80, Scanco Medical AG, Bassersdorf, Switzerland) equipped with a 10-μm focal spot microfocus X-ray tu-
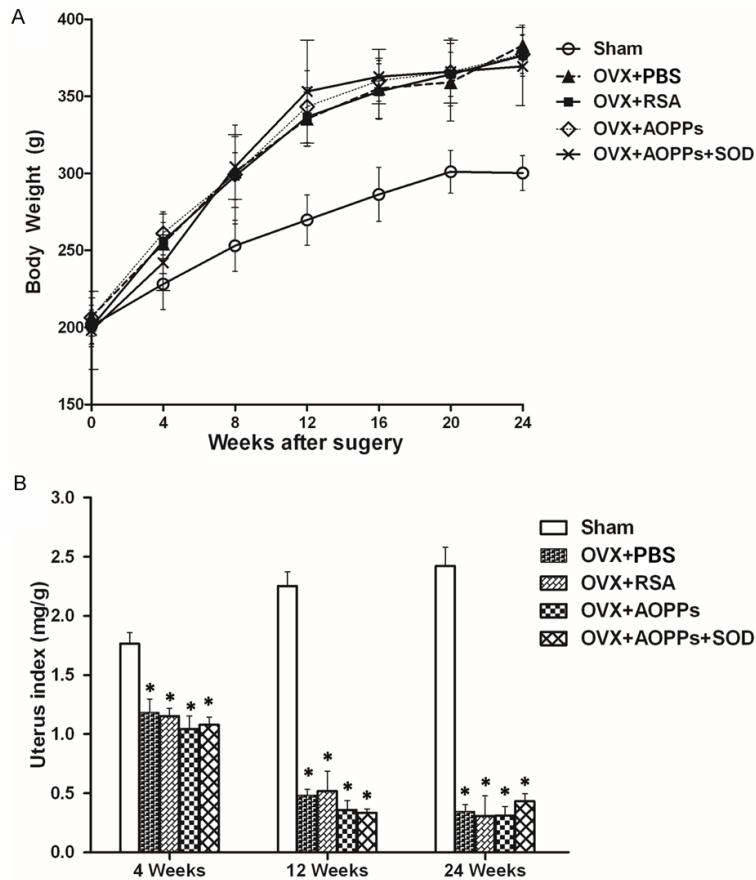
Figure 2. Body weight and uterus index changes in the treatment groups as measured by the electronic scale. A. The body weight of the rats was recorded every 4 weeks during the experimental period. B. Uterus index was represented as uterus weight divide by body weight. Data are presented as mean ± SD, *P < 0.01 compared with the sham group.

at room temperature for 30 min prior to testing and the region of interest, showed as **Figure 1A**, was determined by digital calipers. The samples, continuously moistened with isotonic saline solution during the test, were placed on a base consisting of an aluminium block with one rounded edge-free notches on top (**Figure 1C**). The speed of the feed motion was 2 mm/min with 5% strain rate and the automatic ended by a loss of strength of > 20 N or a linear change of > 2 mm. Data regarding maximum load (Fmax), energy absorption, and stiffness (S) were obtained by Bluehill 2 (version 2.28.832, Instron, a Division of Illinois Tool Works Inc). The experiment was performed blinded with regard to the association between bones and animal groups.

Statistical analysis

Results are expressed as mean ± standard deviation. Statistical differences between different groups for the same time or over the entire period were compared using one-way ANOVA. The homogeneity variances were first compared among the groups. Subsequently, multiple comparisons were performed using the LSD method or Dunnett's C method. The statistical significance was assumed at P < 0.05, and the statistical analyses were conducted with SPSS 13.0 software.

Results

Body weight and uterus index

All the test subjects had a similar initial average body weight, and at week 4, the average body mass of OVX+PBS, OVX+RSA, and OVX+AOPPs groups was significantly higher than that of the sham group (256.0±12.1, P = 0.004; 254.3±19.3 g, P = 0.007; 261.1±14.0 g, P = 0.001; 228.2±16.5g; respectively). The body

be as the source. A 2-mm region of trabecular bone, starting from 2 mm distal to the proximal growth plate (**Figure 1A**), was used for structural evaluation. Low-density foam was used to position the specimen tightly in the sample holder to ensure no relative movement between the specimen and the sample holder during the scan. The resultant grayscale images obtained had an isotropic voxel size of 12 μm, and the X-ray tube was operated at 55 kVp and 49 μA.

Three-point mechanical strength testing

The mechanical properties of the tibia were tested using the three-point bending test describe by Sturmer [26], performed by a miniature Instron material testing machine (Electroplus E1000 Test System) with a 2000-N load cell (**Figure 1C**). The tibiae were thawed
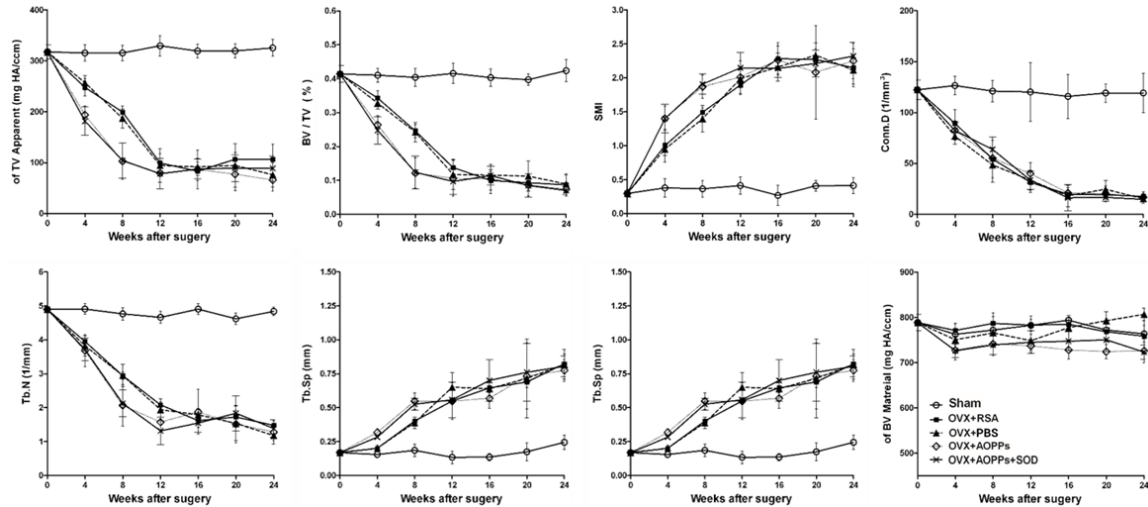
Figure 3. Morphological parameters of trabecular changes throughout the experiment as measured by µCT. Each value was derived from a single serial cross-section obtained from the left tibia of rats. Data are presented as mean ± SD.

mass of the OVX+AOPPs+SOD group at week 4 was 241.9±17.9 g, which was not significantly different from that of the sham group (P = 0.155). The body mass of all the groups increased steadily with age, as expected, and from 8 to 24 weeks. The OVX+PBS, OVX+RSA, OVX+AOPPs and OVX+AOPPs+SOD groups were significantly heavier than the sham group (P < 0.01). There were no significant differences in body weight between the OVX+PBS and OVX+RSA groups starting from week 4 to the end of experiment. (**Figure 2A**)

The uterus index of OVX rats was lower than that of the sham group (P < 0.01), indicating the uterine tissue of rats without ovaries was atrophic, which proved the success of the surgical procedure (**Figure 2B**).

Micro-computed tomography (µCT)

The changes in trabecular microarchitecture in the tibial metaphyseal region among the various treatment groups measured by µCT are shown in **Figure 3**, and the representative three-dimensional micro-CT reconstructions renderings are illustrated in **Figure 4**. From 4 to 24 weeks, the microarchitectural parameters of groups with OVX surgery (OVX+PBS, OVX+RSA, OVX+AOPPs, OVX+AOPPs+SOD) showed significant difference from the sham group in almost all tested indices (bone volume/tissue volume [BV/TV], TV apparent, stru-

cture model index [SMI], connect density [Conn.D], trabecula number [Tb.N], trabecula thickness [Tb.Th], and trabecular space [Tb. Sp]) (P < 0.05 or 0.01) except the BV material.

TV apparent, BV/TV, Conn.D, Tb.N, and Tb.Th were significantly higher in the sham group, and in contrast, SMI and Tb.Sp were significantly increased in response to OVX (P < 0.01 for all). All the above parameters in the OVX+RSA group exhibited no significant differences from the OVX+PBS group, and the same results were observed between the OVX+AOPPs and OVX+AOPPs+SOD groups. Compared with the sham group, the BV material changed significantly (P < 0.01) at all time points in both OVX+AOPPs and OVX+AOPPs+SOD groups, but in the OVX+PBS group, this parameter showed a significant difference (P < 0.01) only in Week 12 and Week 24.

The damage effect of AOPPs on the trabecular architecture was apparent at week 4 and week 8. Significant changes were detected at 4 weeks and 8 weeks for all the morphological parameters, including TV apparent (-24.6%, P < 0.01 and -45.0%, P < 0.01), BV material (-3.0%, P = 0.031 and -3.2%, P = 0.024), BV/TV (-19.5%, P = 0.021 and -49.4%, P < 0.01), Tb.Th (-22.0%, P < 0.01 and -20.6%, P = 0.047), SMI (+47.9%, P = 0.012 and +33.9%, P = 0.03) and Tb.Sp (+57.6%, P < 0.01 and +40.7%, P < 0.01), except for Conn.D and Tb.N
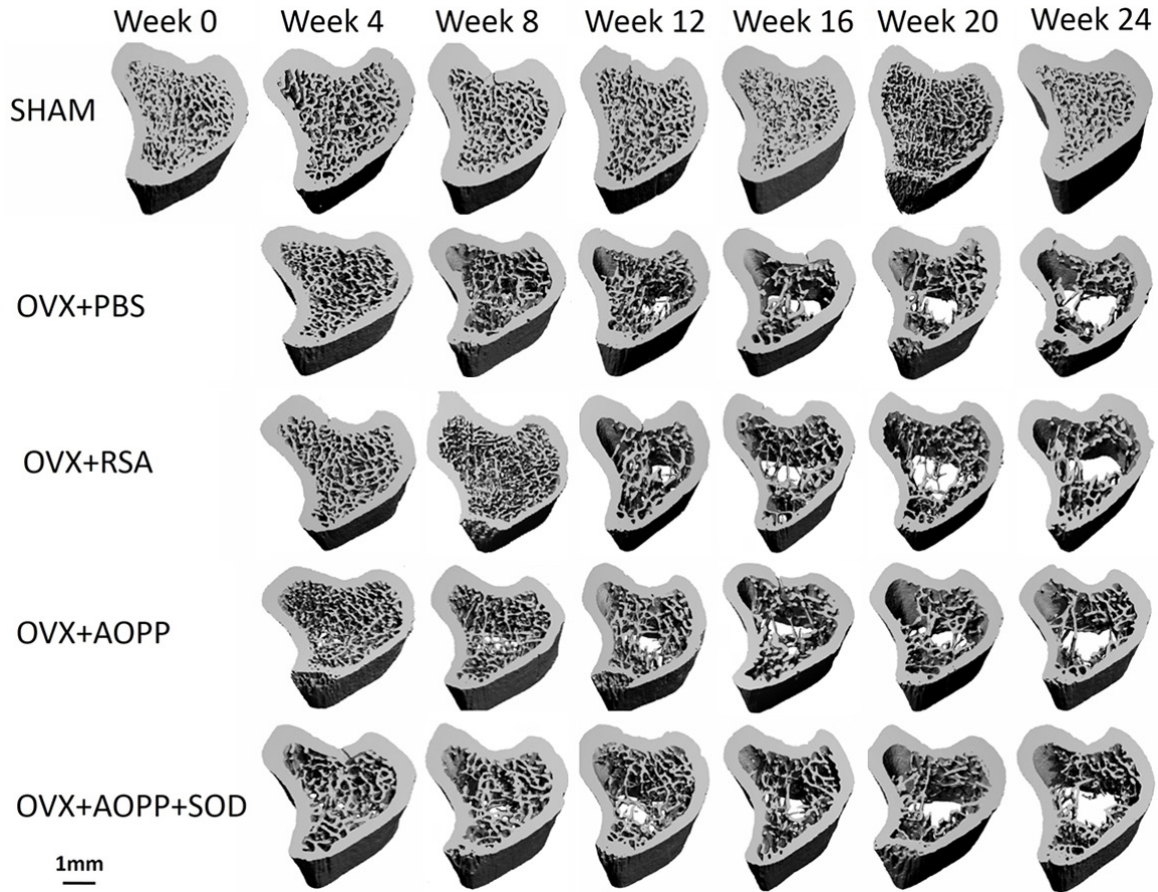
Figure 4. Three-dimensional μCT images of the tibia metaphyseal of sham, OVX+PBS, OVX+RSA, OVX+AOPPs, and OVX+AOPPs+SOD treated Sprague Dawley rat at the time of operation and follow-up measurements 4, 8, 12, 16, 20, and 24 weeks later. Images were chosen from the animals with median cancellous BV/TV values.

in the OVX+AOPPs group compared to that in the OVX+PBS group, respectively. However, in addition to BV material, the structural indices scanned by μCT did not change significantly between the OVX+AOPPs and OVX+PBS groups within 12 to 24 weeks. OVX+AOPPs exhibited significant difference from the OVX+PBS group in BV material for almost all time points except for week 12 and on the contrary no significant difference was found for Conn.D and Tb.N throughout the experiment.

Biomechanical quality of the tibia

The mean maximum load (F_{max}), energy absorption, and stiffness measured from the miniature material testing machine for all the groups at different time points are provided in **Table 1**. As rats became older, F_{max} of the sham group increased from 85.89±8.65 N in week 0 to 140.02±12.33 N at week 24 (+63.0%),

and a significant difference was found at week 8 (P = 0.040), week 16 (P = 0.012), week 20 (P = 0.031) and week 24 (P < 0.001) between the sham and OVX+PBS groups, respectively. Furthermore, there was a significant reduction in F_{max} in the tibia of the OVX+AOPPs group tested by the three-point bend compared to the sham group starting from week 8 to the end of the experiment. However, compared to the OVX+PBS group, 20- and 24-week treatments with AOPPs only markedly decreased the F_{max} (P = 0.001 and 0.002, respectively).

The sham group exhibited a significantly higher energy absorption than OVX+AOPPs from week 8 (P < 0.05 for all), and similarly, the parameter was significantly lower at week 12 (P = 0.007) and week 20 (P = 0.004) compared with OVX+PBS. Only in week 24, a significant difference in energy absorption was observed between OVX+PBS and OVX+AOPPs (P = 0.021).

Table 1. Change of mechanical property at the metaphyseal tibia measured by 3-point bending test. Group averages are expressed as mean ± SD

Group		Week(s) after surgery						
		0	4	8	12	16	20	24
Fmax (N)	Sham	85.89±8.65	87.97±18.11	95.53±9.29	106.78±12.17	124.90±12.08	126.25±15.06	140.02±12.33
	OVX+PBS		75.96±15.39	67.81±12.36[a]	79.30±22.54	83.87±15.76[a]	92.45±9.22[a]	92.20±8.98[a]
	OVX+RSA		76.07±18.37	70.07±19.98	70.25±6.96[a]	73.71±17.14[a]	91.55.10±18.79	88.81±12.03[a]
	OVX+AOPPs		81.20±18.07	56.10±10.61[a]	67.20±16.34[a]	83.94±19.45[a]	59.84±8.28[a+b]	62.00±8.54[a+b]
	OVX+AOPPs+SOD		79.53±32.44	60.84±16.45[a]	59.94±18.84[a]	80.82±26.74	69.28±15.34[a]	60.93±12.45[a+b]
Energy absorption (mJ)	Sham	69.89±10.61	77.68±24.06	72.88±19.93	91.24±7.57	111.62±22.35	119.33±11.31	112.69±16.81
	OVX+PSB		71.54±25.39	55.93±22.65	66.41±8.621[a]	72.54±22.63	86.14±8.42[a]	81.88±15.64
	OVX+RSA		50.87±18.74	42.62±12.98	64.17±9.05[a]	74.08±21.14	84.23±29.22	86.79±15.19
	OVX+AOPPs		65.82±16.91	57.89±29.64	45.53±20.88[a]	55.88±15.56[a]	56.62±21.96[a]	43.22±12.63[a+b]
	OVX+AOPPs+SOD		52.29±21.11	52.52±12.42	55.74±19.49	60.451±20.91	48.40±22.02[a]	45.33±17.40[a]
Stiffness (N/mm)	Sham	109.88±11.86	118.3±13.33	137.16±26.46	140.41±7.27	148.78±8.59	144.45±10.01	162.19±8.06
	OVX+PBS		108.0±21.34	98.80±15.22	90.15±21.36[a]	112.72±25.72	108.02±9.08[a]	104.51±16.14[a]
	OVX+RSA		120.1±14.31	96.15±14.88	95.27±8.56[a]	102.72±17.83[a]	102.41±7.79[a]	105.85±8.37[a]
	OVX+AOPPs		101.9±19.17	74.49±16.62[a]	86.98±15.33[a]	96.00±10.80[a]	89.33±32.96[a]	96.48±11.79[a]
	OVX+AOPPs+SOD		103.1±17.76	82.74±10.01[a]	84.63±17.48[a]	100.54±18.50[a]	94.85±21.46[a]	89.05±8.77[a]

a: Significant difference from SHAM (P < 0.05); b: Significant difference from OVX+PBS (P < 0.05).

Table 2. Quantitative analysis of bone formation (Osteocalcin) and resorption (CTX) markers of serum levels of rats. Values are means ± SD

Group		Week(s) after surgery						
		0	4	8	12	16	20	24
Osteocalcin (ng/mL)	Sham	32.13±1.34	31.29±2.29	25.06±1.95	24.13±2.88	19.63±5.85	16.07±5.84	17.24±2.88
	OVX+PBS		36.36±1.39[a]	32.61±1.40[a]	27.17±2.38	26.23±1.65	25.50±3.01	22.48±1.70
	OVX+RSA		36.87±2.15[a]	33.06±3.93	27.44±1.57	25.67±4.26	26.01±9.03	22.79±4.15
	OVX+AOPPs		42.29±2.47[a+b]	42.42±5.07[a]	38.98±4.71[a+b]	33.25±6.51	36.47±10.41	37.18±2.31[a+b]
	OVX+AOPPs+SOD		43.25±3.11[a+b]	38.71±5.67[a]	37.21±4.15[a+b]	31.47±2.96	33.42±11.16	29.53±1.92[a+b+c]
CTX (ng/mL)	Sham	21.52±1.98	25.40±4.34	33.84±1.24	39.87±1.56	31.21±0.58	28.98±2.34	31.70±1.98
	OVX+PBS		34.85±5.80	40.98±2.25[a]	45.53±2.42[a]	42.97±8.70	42.38±2.65[a]	35.70±1.31
	OVX+RSA		32.01±2.87	41.26±3.46[a]	44.90±4.92	41.12±4.03[a]	46.88±3.65[a]	41.14±3.41[a]
	OVX+AOPPs		37.84±2.63[a]	52.25±2.37[a+b]	52.92±3.37[a+b]	53.25±3.31[a]	48.49±2.63[a]	52.84±3.61[a+b]
	OVX+AOPPs+SOD		33.28±2.80	51.24±2.54[a+b]	51.82±2.01[a+b]	53.97±2.08[a]	50.62±8.61[a]	45.74±2.11[a+b]

a: Significant difference from SHAM (P < 0.05); b: Significant difference from OVX+PBS (P < 0.05); c: Significant difference from OVX+AOPPs (P < 0.05).

Compared with the sham group, OVX+PBS also resulted in a decrease in stiffness at week 12 (P = 0.021), week 20 (P = 0.001) and week 24 (P = 0.001), and treatment with AOPPs could intensify the process because from week 8 to week 24, stiffness in both the OVX+AOPPs and OVX+AOPPs+SOD groups showed a significant difference from the sham group (P < 0.05 for all). However, no statistical differences were found between the OVX+AOPPs and OVX+AOPPs+SOD groups for all the above three parameters throughout the study, and a similar result was observed between the OVX+PBS and OVX+RSA groups.

Biochemical parameters of serum

The results for osteocalcin and CTX-I levels of different groups at different times are given in **Table 2**. The serum osteocalcin level in the OVX+PBS group was significantly elevated compared to that in the sham group at week 4 (P = 0.033) and week 8 (P < 0.01). The OVX+AOPPs group showed significantly higher levels than the sham group at week 4 (P <0.001), week 8 (P = 0.001), week 12 (P = 0.002) and week 24 (P < 0.001) and the same result was observed at week 4 (P = 0.008), week 12 (P = 0.012) and week 24 (P = 0.001) when compared with the OVX+PBS group. Furthermore, the level of OC was reduced in the OVX+AOPPs+SOD group at week 24 compared to that in the OVX+AOPPs group (P = 0.001).

Regarding bone resorption, CTX-I was significantly lower in the sham group than in the OVX+PBS group at 8 weeks (P = 0.002), 12 weeks (P = 0.023) and 24 weeks (P < 0.001) after surgery. Moreover, significant differences were found in the CTX-I levels between the sham group and the OVX+AOPPs group throughout the experiment (P < 0.001 for all), and the OVX+AOPPs group showed a stronger increase in CTX-I levels than the OVX+PBS group at week 8 (P < 0.001), week 12 (P = 0.044) and week 24 (P < 0.001). Throughout the study, no significant difference was observed between the OVX+AOPPs and OVX+AOPPs+SOD groups.

Discussion

Osteoporosis is a disease characterised by reduction in bone mass, microarchitectural deterioration and biomechanical competence of appendicular and axial skeleton, resulting in increased incidence of fractures [27]. The most common type of osteoporosis is postmenopausal osteoporosis. Ovariectomy-induced osteopenia in the rat produces skeletal responses similar to that in postmenopausal women; therefore, the OVX rat is considered to be a gold standard model for evaluating drugs or other materials for the prevention or acceleration of osteoporosis [28]. Besides, the OVX rat model was also recommended by the U.S. Food and Drug Administration (FDA) for feasibility studies assessing the antiosteoporotic efficacy of antiresorptive and anabolic agents [29]. To discuss the relationship between AOPPs, a novel biomarker of oxidative stress, and postmenopausal osteoporosis, we investigated the effects of AOPP-induced OVX rat model and the efficacy of antioxidant SOD in terms of morphological and biomechanical analyses.

AOPPs are a type of dityrosine-containing and cross-linking protein products formed during oxidative stress by the reaction of plasma albumin with chlorinated oxidants [14]; in the present study, AOPPs were obtained by exposing RSA solution into HOCL. During the process of the reaction, RSA could not be thoroughly consumed and some RSA might be left. Therefore, native RSA solution was daily injected into the rats to determine whether RSA had any effect on the OVX rats. The data presented in the OVX+RSA group showed no significant difference with the OVX+PBS group in almost all the experiment parameters; thus, we concluded that it was AOPPs, not RSA, that caused the difference in the OVX rats.

Quantitative histologic techniques had been the standard for assessing trabecular and cortical bone architecture for a long time [30]. However, histologic analyses had limitations regarding bone microarchitecture because structural parameters are rooted in stereologic analysis of a few two-dimensional sections. Micro-CT, also known as µCT, was first introduced by Feldkamp and colleagues in the late 1980s [31] and has currently become the gold standard for the evaluation of bone morphology and microarchitecture in rats and other small animal models ex vivo because it can measure bone microarchitecture directly without relying on stereologic models as compared to histologic analyses [32]. The type of micro-CT sys-

tem used in this study was µCT80 which could provide bone microarchitecture parameters of TV apparent and BV material besides the traditional parameters such as BV/TV, Tb.Th, Tb.N, Tb.Sp, SMI, and Conn.D. TV apparent is used to describe mean density of the volume of interest and BV material can provide the mean density of trabecular bone in the region of interest.

The uterus index of groups with OVX surgery was lower than that of the sham group, indicating the ovariectomised model established in the study was successful. In addition, the microarchitectural bone parameters of groups with OVX surgery showed significant difference from the sham group in almost all tested indices, which proved that oestrogen deficiency will result in bone mass loss; this was consistent with previous studies [33, 34].

The data obtained by µCT revealed that the damage effect of AOPPs on the trabecular architecture was apparent at week 4 and week 8 compared with the OVX+PBS group, which implied that oestrogen deficiency and AOPPs had combined damage effects on the trabecular bone of the tibia in the OVX+AOPPs group. The bone loss of the tibia in OVX+AOPPs appeared earlier than that of the OVX+PBS group; this indicated that AOPPs accelerated the bone loss in ovariectomised rats. However, the difference was not obvious between the OVX+AOPPs and OVX+PBS groups from 12 weeks to 24 weeks.

Mechanical testing measurement is one of the important methods to evaluate bone strength, and three-point bending test was adopted in this experiment. The tibia samples were placed on a base consisting an aluminium block with one rounded edge-free notches on top; this design prevented slipping or tipping of the tibia under increasing punctual strength (**Figure 1C**). Tibia treated with OVX surgery had significantly lower F_{max}, energy absorption, and stiffness than the sham group, and the differences were more significant in the OVX+AOPPs group. Furthermore, F_{max} of the OVX+PBS group was higher than that of the OVX+AOPPs group in both week 20 and week 24, and in week 24, a significant difference in energy absorption was also found between the two groups. Although the average level of stiffness was much lower in OVX+AOPPs than in the mono-treatment OVX

group, no significant difference was found between them owing to large standard deviation in both the groups. The results of mechanical testing measurement suggested that the rats with OVX surgery showed a decrease in bone strength and that AOPPs could accelerated erosion of the bone.

Both the mechanical testing and µCT measurement showed that AOPPs caused reduction in bone mass and strength. However, the difference between the OVX+AOPPs and OVX+PBS group detected by µCT was at an earlier stage after surgery; when tested by mechanical testing, this situation was detected only in week 20 and week 24. This is because different targets caused different results. The mechanical testing is aimed at the entire tibia, while µCT is focused only on the trabecular bone. As shown in **Figure 3**, there was no major change in the results of µCT from week 12 in both the OVX+AOPPs and OVX+PBS groups, and **Figure 4** shows that after week 12, the volume of interest in the trabecular bone was almost completely destroyed, especially in the middle of this area. Further, in week 20 and week 24, the mechanical properties of the tibia decreased greatly in the OVX+AOPPs group, proving that the damaging effect of AOPPs on the tibia still persisted. Therefore, we concluded that the tibia was affected by AOPPs throughout the study.

From 12 weeks to 24 weeks, the trabecular bone volume was similar between AOPPs and PBS, but there was a difference in bone strength between these two groups, suggesting that there might be a difference in the cortical bone. Therefore, we tested cortical bone by microCT in our next experiment.

Osteocalcin, a noncollagenous protein synthesised by mature osteoblast, is generally regarded as a specific marker of bone formation [35, 36] and CTX-I, a collagen degradation product released by osteoclasts, is considered as a marker of bone resorption [37, 38]. Our previous study demonstrated that exposure of rat osteoblast-like (ROB) cells to AOPPs significantly decreased the expression of the osteocalcin protein in both concentration- and time-dependent manner [24]. However, the biomarker results showed that both osteocalcin and CTX-I were elevated in OVX animals, especially in the OVX+AOPPs group. Lerner [39] reported that in

postmenopausal osteoporosis, bone resorption and bone formation were increased, and the reason for increase in the osteocalcin level was not because individual osteoblasts produced more osteocalcin but because of the increase in the number of bone-forming osteoblasts. Our findings are consistent with this result, and therefore, we believe that AOPPs could elevate the number of active osteoblasts and osteoclasts that will result in the upregulation of osteocalcin and CTX-I in serum.

SOD, the antioxidant enzyme, can prevent the accumulation of superoxide by converting superoxide to hydrogen peroxide [40]. Increase in AOPPs and MDA and the decrease in SOD were observed in some pathophysiologic processes, including ageing [41] and postmenopausal bone loss [42]. Our previous study had demonstrated that SOD could reverse the AOPP-induced inhibition of ROB cell proliferation and differentiation in vitro [24], and consequently, we thought that SOD could prevent the occurrence and development of osteoporosis induced by AOPPs. However, in contrast to our supposition, the OVX+AOPPs+SOD group did not show any significant difference compared to the OVX+AOPPs group in almost all the experimental results. This result was the same with our previous study that AOPPs increase bone loss in rats and the progress could not be altered by the antioxidant enzyme, SOD [43]. The effect of AOPPs was reversed by SOD in vitro; however, this does not imply that the same result could be obtained in vivo. The exact mechanism of AOPPs' effect on osteoporosis needs further investigation.

Our study discussed the alteration in tibial bone mass from 4 weeks to 24 weeks with or without intervention. To the best of our knowledge, few studies have investigated the change in tibial bone mass for such a long time by using μCT. Therefore, our results could offer some reference to other researchers interested in studying bone mass loss of the OVX model.

Conclusion

This study demonstrated that AOPPs accelerated bone loss and weakened bone strength in the OVX rat model, and this process could not be prevented by the antioxidant enzyme SOD. These results suggested that the serum levels of AOPPs, a novel biomarker of oxidative stress, in postmenopausal women might accelerate the development of osteoporosis, which may provide new targets for intervention.

Disclosure of conflict of interest

None.

Address correspondence to: Shuai Zheng and Jian-Ting Chen, Department of Spinal Surgery, NanFang Hospital, Southern Medical University, 1838 North Guangzhou Avenue, Guangzhou, China. Tel: +8620-61641723; Fax: +86-20-61641721; E-mail: zhengshuai041@qq.com (SZ); chenjt99@tom.com (JTC)

References

[1] Brunader R, Shelton DK. Radiologic bone assessment in the evaluation of osteoporosis. Am Fam Physician 2002; 65: 1357-1364.

[2] Valli A, Suliman ME, Meert N, Vanholder R, Lindholm B, Stenvinkel P, Watanabe M, Barany P, Alvestrand A, Anderstam B. Overestimation of advanced oxidation protein products in uremic plasma due to presence of triglycerides and other endogenous factors. Clin Chim Acta 2007; 379: 87-94.

[3] Garrett IR, Boyce BF, Oreffo RO, Bonewald L, Poser J, Mundy GR. Oxygen-derived free radicals stimulate osteoclastic bone resorption in rodent bone in vitro and in vivo. J Clin Invest 1990; 85: 632-639.

[4] Zhang Y, Zhong Z, Hou G, Jiang H, Chen J. Involvement of oxidative stress in age-related bone loss. J Surg Res 2011; 169: e37-e42.

[5] Stanojkovic I, Kotur-Stevuljevic J, Milenkovic B, Spasic S, Vujic T, Stefanovic A, Llic A, Ivanisevic J. Pulmonary function, oxidative stress and inflammatory markers in severe COPD exacerbation. Respir Med 2011; 105 Suppl 1: S31-S37.

[6] Kotur-Stevuljevic J, Memon L, Stefanovic A, Spasic S, Spasojevic-Kalimanovska V, Bogavac-Stanojevic N, Kalimanovska-Ostric D, Jelić-

Ivanovic Z, Zunic G. Correlation of oxidative stress parameters and inflammatory markers in coronary artery disease patients. Clin Biochem 2007; 40: 181-187.

[7] Powers SK, Smuder AJ, Judge AR. Oxidative stress and disuse muscle atrophy: cause or consequence? Curr Opin Clin Nutr Metab Care 2012; 15: 240-245.

[8] Cabiscol E, Piulats E, Echave P, Herrero E, Ros J. Oxidative stress promotes specific protein damage in Saccharomyces cerevisiae. J Biol Chem 2000; 275: 27393-27398.

[9] Karihtala P, Soini Y. Reactive oxygen species and antioxidant mechanisms in human tissues and their relation to malignancies. APMIS 2007; 115: 81-103.

[10] Valentine JS, Wertz DL, Lyons TJ, Liou LL, Goto JJ, Gralla EB. The dark side of dioxygen biochemistry. Curr Opin Chem Biol 1998; 2: 253-262.

[11] DeAtley SM, Aksenov MY, Aksenova MV, Carney JM, Butterfield DA. Adriamycin induces protein oxidation in erythrocyte membranes. Pharmacol Toxicol 1998; 83: 62-68.

[12] Piwowar A, Knapik-Kordecka M, Warwas M. AOPP and its relations with selected markers of oxidative/antioxidative system in type 2 diabetes mellitus. Diabetes Res Clin Pract 2007; 77: 188-192.

[13] Witko-Sarsat V, Friedlander M, Capeillère-Blandin C, Nguyen-Khoa T, Nguyen AT, Zingraff J, Jungers P, Descamps-Latscha B. Advanced oxidation protein products as a novel marker of oxidative stress in uremia. Kidney Int 1996; 49: 1304-1313.

[14] Witko-Sarsat V, Friedlander M, Nguyen Khoa T, Capeillère-Blandin C, Nguyen AT, Canteloup S, Dayer JM, Jungers P, Drüeke T, Descamps-Latscha B. Advanced oxidation protein products as novel mediators of inflammation and monocyte activation in chronic renal failure. J Immunol 1998; 161: 2524-2532.

[15] Kalousova M, Zima T, Tesar V, Lachmanova J. Advanced glycation end products and advanced oxidation protein products in hemodialyzed patients. Blood Purif 2002; 20: 531-536.

[16] Atabek ME, Keskin M, Yazici C, Kendirci M, Hatipoglu N, Koklu E, Kurtoglu S. Protein oxidation in obesity and insulin resistance. Eur J Pediatr 2006; 165: 753-756.

[17] Krzystek-Korpacka M, Neubauer K, Berdowska I, Boehm D, Zielinski B, Petryszyn P, Terlecki G, Paradowski L, Gamian A. Enhanced formation of advanced oxidation protein products in IBD. Inflamm Bowel Dis 2008; 14: 794-802.

[18] Kocak H, Oner-Iyidoğan Y, Gürdöl F, Oner P, Süzme R, Esin D, Işsever H. Advanced oxidation protein products in obese women: its relation to insulin resistance and resistin. Clin Exp Med 2007; 7: 173-178.

[19] Chen Y, Nixon NB, Dawes PT, Mattey DL. Influence of variations across the MMP-1 and -3 genes on the serum levels of MMP-1 and -3 and disease activity in rheumatoid arthritis. Genes Immun 2012; 13: 29-37.

[20] Zhou QG, Zhou M, Lou AJ, Xie D, Hou FF. Advanced oxidation protein products induce inflammatory response and insulin resistance in cultured adipocytes via induction of endoplasmic reticulum stress. Cell Physiol Biochem 2010; 26: 775-786.

[21] Wei XF, Zhou QG, Hou FF, Liu BY, Liang M. Advanced oxidation protein products induce mesangial cell perturbation through PKC-dependent activation of NADPH oxidase. Am J Physiol Renal Physiol 2009; 296: F427-F437.

[22] Zhou LL, Hou FF, Wang GB, Yang F, Xie D, Wang YP, Tian JW. Accumulation of advanced oxidation protein products induces podocyte apoptosis and deletion through NADPH-dependent mechanisms. Kidney Int 2009; 76: 1148-1160.

[23] Zhou QG, Peng X, Hu LL, Xie D, Zhou M, Hou FF. Advanced oxidation protein products inhibit differentiation and activate inflammation in 3T3-L1 preadipocytes. J Cell Physiol 2010; 225: 42-51.

[24] Zhong ZM, Bai L, Chen JT. Advanced oxidation protein products inhibit proliferation and differentiation of rat osteoblast-like cells via NF-kappaB pathway. Cell Physiol Biochem 2009; 24: 105-114.

[25] Li HY, Hou FF, Zhang X, Chen PY, Liu SX, Feng JX, Liu ZQ, Shan YX, Wang GB, Zhou ZM, Tian JW, Xie D. Advanced oxidation protein products accelerate renal fibrosis in a remnant kidney model. J Am Soc Nephrol 2007; 18: 528-538.

[26] Sturmer EK, Seidlová-Wuttke D, Sehmisch S, Rack T, Wille J, Frosch KH, Wuttke W, Stürmer KM. Standardized bending and breaking test for the normal and osteoporotic metaphyseal tibias of the rat: effect of estradiol, testosterone, and raloxifene. J Bone Miner Res 2006; 21: 89-96.

[27] Kanis JA. Diagnosis of osteoporosis and assessment of fracture risk. Lancet 2002; 359: 1929-1936.

[28] Kharode YP, Sharp MC, Bodine PV. Utility of the ovariectomized rat as a model for human osteoporosis in drug discovery. Methods Mol Biol 2008; 455: 111-124.

[29] Thompson DD, Simmons HA, Pirie CM, Ke HZ. FDA Guidelines and animal models for osteoporosis. Bone 1995; 17: 125S-133S.

[30] Parfitt AM. Bone histomorphometry: proposed system for standardization of nomenclature,

symbols, and units. Calcif Tissue Int 1988; 42: 284-286.

[31] Feldkamp LA, Goldstein SA, Parfitt AM, Jesion G, Kleerekoper M. The direct examination of three-dimensional bone architecture in vitro by computed tomography. J Bone Miner Res 1989; 4: 3-11.

[32] Bouxsein ML, Boyd SK, Christiansen BA, Guldberg RE, Jepsen KJ, Müller R. Guidelines for assessment of bone microstructure in rodents using micro-computed tomography. J Bone Miner Res 2010; 25: 1468-1486.

[33] Bouxsein ML, Myers KS, Shultz KL, Donahue LR, Rosen CJ, Beamer WG. Ovariectomy-induced bone loss varies among inbred strains of mice. J Bone Miner Res 2005; 20: 1085-1092.

[34] Laib A, Kumer JL, Majumdar S, Lane NE. The temporal changes of trabecular architecture in ovariectomized rats assessed by MicroCT. Osteoporos Int 2001; 12: 936-941.

[35] Akesson K, Ljunghall S, Jonsson B, Sernbo I, Johnell O, Gärdsell P, Obrant KJ. Assessment of biochemical markers of bone metabolism in relation to the occurrence of fracture: a retrospective and prospective population-based study of women. J Bone Miner Res 1995; 10: 1823-1829.

[36] Valimaki MJ, Farrerons-Minguella J, Halse J, Kröger H, Maroni M, Mulder H, Muñoz-Torres M, Sääf M, Snorre Øfjord E. Effects of risedronate 5 mg/d on bone mineral density and bone turnover markers in late-postmenopausal women with osteopenia: a multinational, 24-month, randomized, double-blind, placebo-controlled, parallel-group, phase III trial. Clin Ther 2007; 29: 1937-1949.

[37] Calvo MS, Eyre DR, Gundberg CM. Molecular basis and clinical application of biological markers of bone turnover. Endocr Rev 1996; 17: 333-368.

[38] Rosen HN, Moses AC, Garber J, Iloputaife ID, Ross DS, Lee SL, Greenspan SL. Serum CTX: a new marker of bone resorption that shows treatment effect more often than other markers because of low coefficient of variability and large changes with bisphosphonate therapy. Calcif Tissue Int 2000; 66: 100-103.

[39] Lerner UH. Bone remodeling in post-menopausal osteoporosis. J Dent Res 2006; 85: 584-595.

[40] Keller JN, Kindy MS, Holtsberg FW, St Clair DK, Yen HC, Germeyer A, Steiner SM, Bruce-Keller AJ, Hutchins JB, Mattson MP. Mitochondrial manganese superoxide dismutase prevents neural apoptosis and reduces ischemic brain injury: suppression of peroxynitrite production, lipid peroxidation, and mitochondrial dysfunction. J Neurosci 1998; 18: 687-697.

[41] Linnane AW, Eastwood H. Cellular redox regulation and prooxidant signaling systems: a new perspective on the free radical theory of aging. Ann N Y Acad Sci 2006; 1067: 47-55.

[42] Sendur OF, Turan Y, Tastaban E, Serter M. Antioxidant status in patients with osteoporosis: a controlled study. Joint Bone Spine 2009; 76: 514-518.

[43] Zeng JH, Zhong ZM, Li XD, Wu Q, Zheng S, Zhou J, Ye WB, Xie F, Wu XH, Huang ZP, Chen JT. Advanced oxidation protein products (AOPPs) accelerate bone loss in rats. Int J Clin Exp Pathol 2016; 9: 11289-11300.